Dynamics of Intraseasonal Sea Level Variations Observed at Gan Island and Sibolga

Iskhaq Iskandar
Jurusan Fisika, Fakultas Matematika dan Ilmu Pengetahuan Alam,
Universitas Sriwijaya
e-mail: iskhaq.iskandar@gmail.com

Received 29 June 2009, accepted for publication 28 July 2009

Abstract

Dynamics of intraseasonal sea level variability in the central and eastern equatorial Indian Ocean is examined using 66 months (1 January 1993 to 30 June 1998) of the observed sea level at Gan Island (0°41'S, 73°E) and Sibolga (1°45'N, 98°46'E). The analysis shows that the intraseasonal signals of 20-100-day at those two tidal stations are coherent and exhibit eastward energy propagation. These intraseasonal variations are associated with the propagation of equatorial Kelvin waves generated by the zonal winds along the equator. The lag-correlation analysis reveals that their phase speed is closed to the theoretical phase speed of the first and second baroclinic modes of the Kelvin waves.

Keywords: Gan Island, Indian Ocean, Intraseasonal variation, Kelvin waves, Sea level, Sibolga

Abstrak

Studi ini mengkaji dinamika variasi tinggi muka laut dalam rentang intra-musim di sepanjang ekuator Samudera Hindia menggunakan data pasang surut yang terekam di stasiun Gan Island (0°41'S, 73°E) and Sibolga (1°45'N, 98°46'E) selama kurun waktu 66 bulan dari tanggal 1 January 1993 hingga 30 Juni 1998. Hasil analisis ini menerangkan bahwa sinyal intra-musim dalam periode 20-100-hari yang terekam di kedua stasiun pasang surut tersebut koheren dan menunjukkan adanya perambatan energi kearah timur. Variasi intra-musim ini berasosiasi dengan perambatan gelombang ekuator-Kelvin yang di gerakkan oleh angin baratan disepanjang ekuator. Sementara itu, hasil analisis dengan menggunakan korelasi-silang menunjukkan bahwa kecepatan phase penjalaran sinyal intra-musim ini sesuai dengan kecepatan phase gelombang Kelvin untuk mode baroklinik satu dan dua.

Kata kunci: Pulau Gan, Samudera Hindia, Variasi intra-musim, Gelombang Kelvin, Tinggi muka laut, Sibolga

1. Introduction

Intraseasonal variability (ISV) in the tropical atmosphere at period of about 40-50 days has been the subject of many papers since the seminal work by *Madden and Julian* (1971). They suggested that this variation was of global scale and had aspects suggesting an eastward-propagating wave. Atmospheric ISV generated in the equatorial Indian Ocean can propagate poleward, causing active and break phases of the Asian-Australian monsoon, as well as eastward to the Pacific Ocean to affect El Niño-Southern Oscillation (ENSO).

Indications of an oceanic response to the atmospheric ISV have been observed at many locations in the Indian and Pacific Oceans, extending from the tropics to mid-latitudes. In particular, previous studies in the Indian Ocean have revealed the existence of oceanic ISV on the observed currents in the western equatorial Indian Ocean (*Luyten and Roemmich*, 1982), in the central equatorial Indian Ocean (*McPhaden*, 1982; *Reppin et al*., 1999) as well in the eastern equatorial Indian Ocean (*Masumoto et al*, 2005; *Iskandar et al*., 2008).

Nevertheless, observed sea level along the southeastern boundary of the Indian Ocean shows that there is strong oceanic ISV at period of about 20–90-days (*Arief and Murray,* 1996; *Iskandar et al*., 2005). It was suggested that both remote winds over the equatorial Indian Ocean and alongshore winds along the southern coast of Sumatra and Java play significant role in generating the intraseasonal signals in the observed sea level. In the far-eastern Indian Ocean, oceanic ISV has also been observed in five outflow straits in the Indonesian Throughflow (ITF) region (*Chong et al*., 2000). This ISV has been traced to the equatorial Kelvin waves which are generated by intraseasonal winds in the equatorial Indian Ocean.

The works of *Arief and Murray* (1996), *Iskandar et al* (2005) and *Chong et al* (2000) have brought to light and clarified the large-scale, spatially coherence nature of the poleward-propagating oceanic ISV along the southeastern boundary of the Indian Ocean. However, to our knowledge there is no study which reports intraseasonal coherence of oceanic variability in the equatorial Indian Ocean and along the northeastern boundary of the Indian Ocean.

This study investigates the coherence ISV of sea level observed in the central Indian Ocean at Gan Island (0°41'S, 73°E) and in the northeastern Indian

Ocean at Sibolga (1°45'N, 98°46'E). A brief description of the data and method used in this study is presented in the next section. This is then followed by description of the characteristics of ISV at those two locations. Possible relation between the ISV at those two locations is also examined in this section. The following section discusses the dynamics of this ISV based on the equatorial wave dynamics. The last section is reserved for summarizing the main finding in this study.

2. Data collections and analyses

Primarily data used in this study are daily sea level data recorded at two tidal stations in the Gan Island and Sibolga (Figure 1). The data are obtained from the University of Hawaii Sea Level Center (http://ilikai.soest.hawaii.edu/uhslc/) which covers a period from 1 January 1993 through 30 June 1998. Short gaps up to a few days in length were bridged by applying a linear interpolation in time.

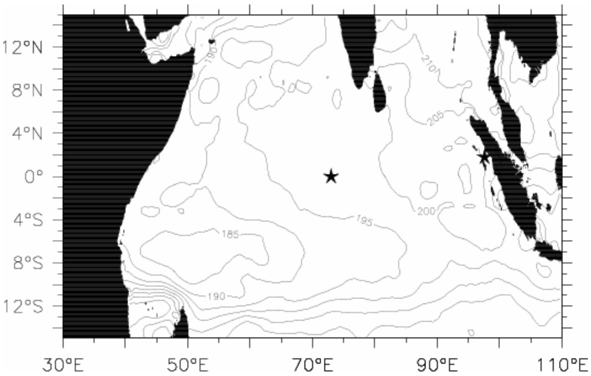

Figure 1. Location of tidal stations used in this study (marked by "*star*"). Gan Island (0°41'S, 73°E) and Sibolga (1°45'N, 98°46'E). The contours indicate the mean absolute dynamic topography for 1993-1997.

In order to evaluate the dynamics of the intraseasonal coherency in the central equatorial and northeastern boundary of the Indian Ocean, satellite product of sea surface high (SSH) and surface winds are used in this study. Multi-missions gridded SSH are obtained from Archiving, Validation and Interpretation of Satellite Oceanography data (AVISO). The horizontal resolution is regularly 1/3° × 1/3° on a Mercator grid, while the temporal resolution is 7 days. The data are available at http://www.aviso. oceanobs.com. Mean while, daily surface winds with spatial resolution of 2.5° are derived from the National Center for Environmental Prediction and the National Center for Atmospheric Research (NCEP/NCAR) reanalysis (http://www.cdc.noaa.gov/data). Note that both gridded SSH and surface winds are analyzed for the same period as the tide-gauge data from 1 January 1993 to 30 June 1998.

For isolating the dominant period of intraseasonal variations, the wavelet spectrum analysis is applied to the observed sea level at each tidal stations. A brief description of the wavelet spectrum analysis is given in the following. Readers are referred to *Torence and Compo* (1998) for further details on wavelet analysis. The continuous wavelet transform of a time series $X(t)$, is defined as

$$W(s,t) = s^{-1/2} \int_{-\infty}^{\infty} X(t')\psi^* \left(\frac{t'-t}{s} \right) dt', \tag{1}$$

which is the convolution of $X(t)$ with a family of functions, $\psi_{st}(t')$, given by

$$\psi_{st}(t') = s^{-1/2} \psi \left(\frac{t'-t}{s} \right). \tag{2}$$

The asterisk (*) in Equation (1) indicates the complex conjugate. s and t represent scale and translation in time, respectively. $\psi(t)$ is the mother wavelet.

In this study, the Morlet wavelet is used for ψ (t), which is defined as

$$\psi(t) = \pi^{-1/4} e^{(imt)} e^{(-t^2/2)}, \tag{3}$$

where m = 6 has been chosen to satisfy the admissibility condition,

$$\int_{-\infty}^{\infty} \psi(t) dt = 0 . \tag{4}$$

The wavelet coherency is a useful method for evaluating the relationships between the oceanic intraseasonal variations in the eastern equatorial Indian Ocean and in the throughflow straits. Following *Torrence and Compo* [1998], we defined the wavelet squared coherency of two time series, $X(t)$ and $Y(t)$, as

$$R^2(s,t) = \frac{\left| \left\langle s^{-1} W^{XY}(s,t) \right\rangle \right|^2}{\left\langle s^{-1} \left| W^X(s,t) \right|^2 \right\rangle \left\langle s^{-1} \left| W^Y(s,t) \right|^2 \right\rangle}, \tag{5}$$

where $\langle \cdot \rangle$ is a smoothing operator in both time and scale. $W^X(s,t)$ and $W^Y(s,t)$ are the wavelet transform of the time series $X(t)$ and $Y(t)$, respectively. $W^{XY}(s)$ is the cross-wavelet spectrum of $X(t)$ and $Y(t)$, which is defined as

$$W^{XY}(s,t) = W^X(s,t) \ W^{Y*}(s,t) . \tag{6}$$

The wavelet-coherence phase difference is given by

$$\Phi(s,t) = \tan^{-1}\left(\frac{\mathrm{Im}\left\{\left\langle s^{-1}W^{XY}(s,t)\right\rangle\right\}}{\mathrm{Re}\left\{\left\langle s^{-1}W^{XY}(s,t)\right\rangle\right\}}\right). \qquad (7)$$

The wavelet coherence gives a measure of the correlation between the two time series as a function of both scale and time. Note that throughout this paper, the term "coherency" indicates the wavelet squared coherency. The wavelet phase, on the other hand, measure the phase difference between the complex wavelet transforms and indicates the presence of any lag or lead relationship between the two time series. This term is also as function of scale and time.

3. Temporal characteristics of the observed sea level

Deviations from the mean of the observed sea level at Gan Island and Sibolga are presented in Figure 2. For clarity, the time series were smoothed with a 11-day running-mean for this presentation only. However, the rest of the analysis uses the unsmoothed time series.

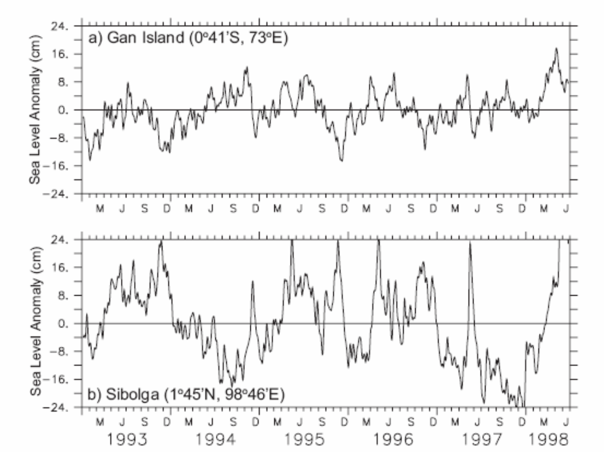

Figure 2. Time series of the observed sea level anomaly at (a) Gan Island and (b) Sibolga for 1 January 1993 to 30 June 1998. Note that the anomaly is deviation from time mean of 1993-1998 and the time series were smoothed with a 11-day running mean.

It is shown that the amplitude of sea level variation at Gan Island is smaller than that observed at Sibolga. Moreover, a strong semiannual cycle is clearly evident at Sibolga compares to that at Gan Island. This semiannual signal, showing positive sea level anomaly (SLA) during April-May and October-November, is associated with the semiannual Wyrtki jet (*Wyrtki*, 1973). The observed sea level also indicates interannual variation: it is anomalously very low (high) at Sibolga (Gan Island) during July – October 1994 and July 1997 – February 1998. The lowering (increasing) of sea level at Sibolga (Gan Island) was associated with an inherent coupled climate mode in the tropical Indian Ocean, so-called the Indian Ocean Dipole (IOD; *Saji et al*., 1999; *Webster et al*., 1999; *Murtugudde et al*., 2000). It has been suggested that the IOD event develops via feedbacks between zonal wind stress, sea surface temperature (SST) and thermocline depth anomalies. The positive IOD event is characterized by cold (low) SST (sea level) anomalies in the southeastern tropical basin, accompanied by warm (high) SST (sea level) anomalies in the western tropical basin

In order to isolate the dominant period of the ISV, we have calculated the wavelet spectrum of the observed sea level at Gan Island and Sibolga (Figure 3). Pronounced ISV with period of about 50-100 days is clearly observed at Gan Island (Figure 3a) almost throughout the period of observation. Strong intraseasonal signals are observed during August 1994 through October 1997. The spectral peak shifted to somewhat shorter period of about 30–60 days during March-July 1993. On the other hand, the ISV did not appear from November 1997 to the end of the observational period.

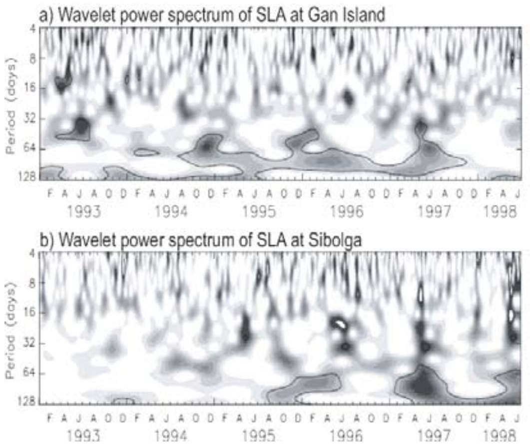

Figure 3. The Morlet wavelet spectra of the observed sea level at a) Gan Island and (b) Sibolga being normalized by the global wavelet spectra. The thick-black contours correspond to the 95% confidence level.

The wavelet power spectra of the sea level at Sibolga also reveal intraseasonal variations (Figure 3b). Strong ISV with period of about 50-100 days, however, is only observed during August 1995 to June 1996 and from February 1997 through the end of the observational period. During 1993 and 1994, the observed sea level also revealed some energetic ISV, though it is below the 95% confidence level.

The inter-relation of the ISV signals observed at Gan Island and those observed at Sibolga is, then, examined by calculating the wavelet coherency (Figure 4). The most notable feature captured by the wavelet coherency is a significant coherency in intraseasonal time-scale of about 20-100-day band, while another intriguing feature is distinct coherency within biweekly time-scale of about 6-16-day band. However, we do not discuss further the biweekly signal in this study and will be a subject of our future study. We also note an interannual modulation, which appears as an interval of low coherency during November 1993-September 1994 and November 1997 through the end of the observation. These two intervals of low coherency are coincident with the IOD events of 1994 and 1997/98.

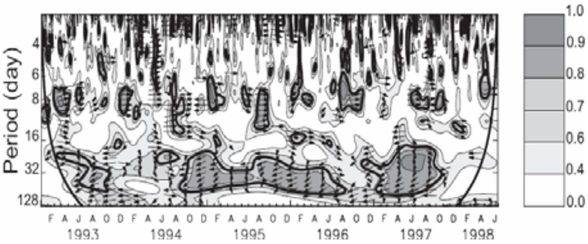

Figure 4. The wavelet coherency between the observed sea level at Gan Island and Sibolga. The relative phase relationship is shown as arrows, with in phase pointing right, anti-phase pointing left, and the first time series leading the second one by 90° pointing straight down. The thick-black contour is the 95% confidence level.

There are also interesting features in the wavelet coherency of the two time series, such as significant coherency within biweekly time-scale throughout the observational period. The wavelet power spectra of the two time series (Figures 3a-b), however, show low power within this period band. In addition, there is also strong coherency in the intraseasonal time-scale during April-October 1993 and October 1994-July 1995, though the wavelet power spectrum of the sea level at Sibolga (Figure 3b) shows minimal power. The significant regions within those two period-bands are so extensive that is it very unlikely that those are simply by chance. These results, therefore, suggest that event during times of low relationship between the signals at those two tidal stations, the signals can still show occasional strong interaction.

To evaluate the phase relation of the observed ISV at those two tidal stations, we investigate the vectors in Figure 4, which indicate the phase difference between the observed sea level at Gan Island and that at Sibolga at each time and period. One can clearly see that within the intraseasonal time-scale (20-100-day) the signals at Gan Island lead those at Sibolga by about 120°. This implies that it takes about 15 days for a 60-day signal to radiate its energy from Gan Island to Sibolga. Note that this phase difference appears almost constant over the 1993-1997 record.

To confirm the above relation, we have calculated the correlation between the sea levels observed at those two tidal stations for the 20–100-day band-passed data (Figure 5). The result shows that the peak correlation is obtained when the signals at Gan Island lead those at Sibolga by 11 days. The phase speed estimated from this lag-correlation analysis is about 3.04 ms^{-1}, which is close to the observed phase speed of the first baroclinic mode of Kelvin wave (2.86 ms^{-1}) derived from the mean density profile of the World Ocean Atlas 2001 for the Indian Ocean.

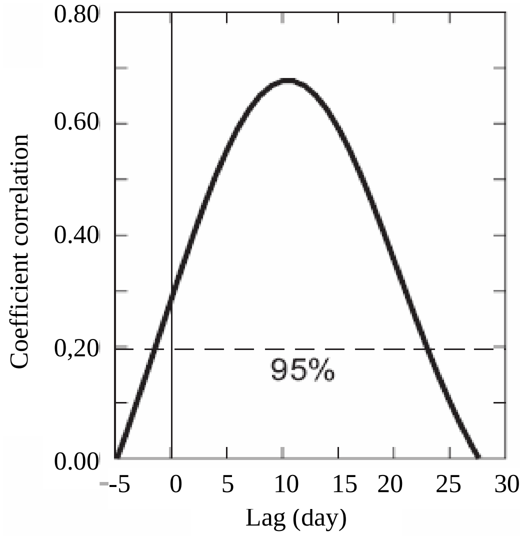

Figure 5. Lagged-correlation coefficients of 20–100-day band-passed sea level at Gan Island and Sibolga. The horizontal dashed-line indicates the 95% confidence level using *t*-test.

In order to evaluate the forcing region of this oceanic ISV, the correlation between the observed sea level at Sibolga and the zonal winds for 20–100-day band-passed data is calculated (Figure 6). The result shows that the sea level at Sibolga has high correlation with the zonal winds when the former lag the latter by about 12 days. This indicates that the remote forcing from the central equatorial Indian Ocean plays an important role in generating the intraseasonal signals observed at Sibolga, though local forcing from the alongshore winds may be a contributing factor.

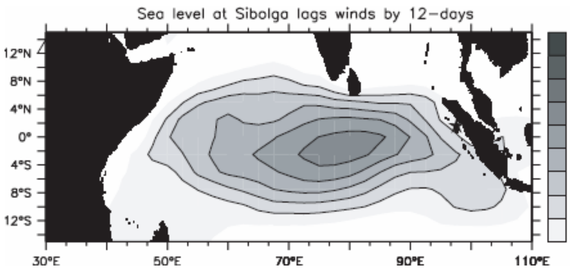

Figure 6. Correlation map between the zonal winds and the observed sea level at Sibolga for 20–100-day band-passed data. The correlations above 95% confidence level are contoured.

4. Discussion

Using wavelet analysis, it was shown that there is a relationship between intraseasonal signal in the Gan Island and that in the Sibolga. However, the mechanism responsible for the link between those two signals is not yet clear. In this section, therefore, we discuss the dynamics relating the signals at those two tidal stations using the satellite observed SSH along the equator.

First, in order to separate intraseasonal signals, the SSH along the equator was band-pass filtered using the complex Morlet wavelet transform within 20–100-day (*Torrence and Compo*, 1998). The resulting filtered SSH is plotted in Figure 7 from January 1993 to June 1998. Note that for clarity we have applied a 5° running mean for the zonal direction. An examination of the longitude-time diagram reveal eastward propagating signal. The intraseasonal signals are propagating almost all the time except during part of 1993 and 1997. In addition, it is also shown that the maximum amplitudes of variability are found in the central and eastern basin.

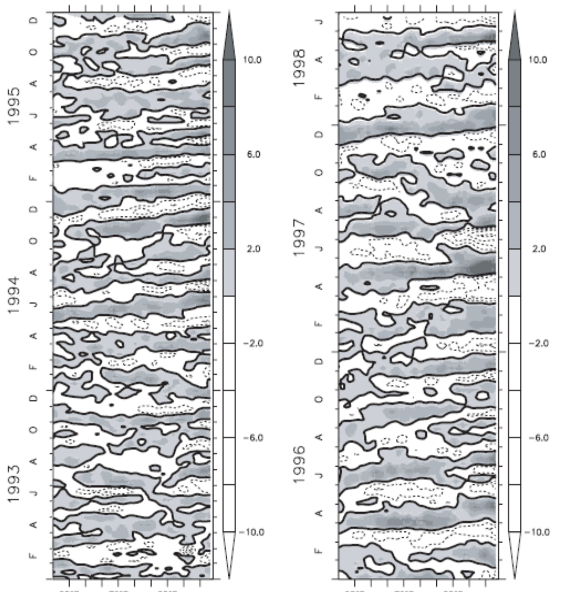

Figure 7. Longitude-time diagram of the 20–100-day band-passed sea surface height along the equator. A 5° running mean is applied for the zonal direction.

The estimation for phase speed of these propagating band-pass filtered signals, was conducted by calculating lag correlations between the filtered time series at 98°E and those at other longitudes along the equator for the period of January 1993 to June 1998 period. The result shows that the signal observed at 98°E lags that at 65°E by about 3 weeks (Figure 8). This indicates an eastward propagating-signal with a phase speed of about 2.1 ms^{-1}. The estimated phase speed from the lag-correlation analysis performed on the bad-passed filtered satellite SSH, but falls between the theoretical values of the first (2.86 ms^{-1}) and the second (1.8 ms^{-1}) baroclinic modes of Kelvin waves derived from the mean density profiles of the World Ocean Atlas 2001. This result may indicate that both modes are present in the 20–100 days oceanic variations in the equatorial Indian Ocean. This is in agreement with the previous observational (*Fu*, 2006) and numerical (*Han*, 2005) studies.

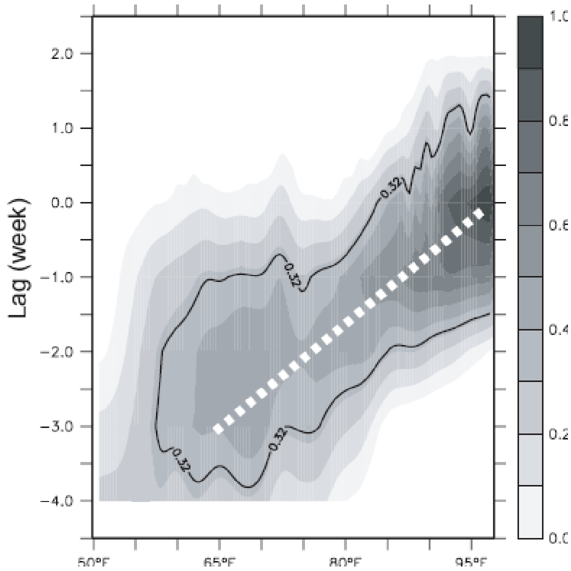

Figure 8. Lag-correlation diagram between filtered time series of satellite observed sea surface height (SSH) at 98°E and those at other longitudes along the equator. Negative lag indicates the SSH variability at 98°E lags to those at other points along the equator. White-dashed line is approximate trajectory of the filtered SSH. The 95% confidence level is marked by black contours.

It is recently shown that the variability of the intraseasonal winds over the equatorial Indian Ocean is modulated by the IOD on interannual timescales (*Rao and Yamagata*, 2004; *Han et al.*, 2006). This suggests existence of interesting scale-interactions among shorter- and longer-period phenomena in the tropical Indian Ocean. During the IOD event, the westerly zonal winds are anomalously weakened or even reverse the direction (*Saji et al.*, 1999). This leads to absence of the eastward equatorial oceanic jets in the Indian Ocean and contributes to lowering (shoaling) sea level (thermocline) in the eastern Indian Ocean and rising (deepening) sea level (thermocline) in the western Indian Ocean (*Vinayachandran et al.*, 1999; *Murtugudde et al.*, 2000). Our result (Figure 2) has shown that the IOD events in 1994 and 1997 clearly affected the sea level at those two tidal stations. The observed sea level at Gan Island indicates positive anomaly during 1994 and 1997 IOD event, while that at Sibolga station shows negative anomaly. Moreover, the wavelet analysis on the observed sea level (Figure 3) shows that the intraseasonal variations during the IOD events are weaken (strengthen) at Sibolga (Gan Island).

5. Conclusion

This study examined the intraseasonal sea level variations observed at Gan Island and Sibolga using the wavelet analysis. The relationships of the intraseasonal signals observed at those two tidal stations were evaluated based on the equatorial wave dynamics. The results show that there exist robust intraseasonal oceanic variations at a period of 20–100 days in the Gan Island as well as in the Sibolga tidal stations. In the Gan Island tidal station, the intraseasonal variations are apparently observed throughout the time. On the other hand, the intraseasonal variations in the Sibolga tidal station reveal interannual modulation: they are strong during August 1995 to June 1996 and February 1997 through June 1998, but suppressed during other periods the intraseasonal variations.

The wavelet coherency between the sea level observed at Gan Island and that observed at Sibolga demonstrates significant intraseasonal coherency within intraseasonal time-scale. The coherency is still high even though the wavelet power spectrum of the sea level at Sibolga shows minimal power. This indicates that event during times of low relationship between the signals at those two tidal stations, the signals can still show occasional strong interaction.

The phase relationship from the coherence analysis as well as the lag correlation shows that the intraseasonal signals are propagating eastward with phase speed of about 3.04 ms^{-1}. This phase speed is very close to the theoretical phase speed of the first baroclinic Kelvin waves. Thus, it is argued that he intraseasonal coherency between the observed sea level at Gan Island and that at Sibolga is associated with the first baroclinic Kelvin waves which propagate eastward along the equator. Moreover, the lag correlation analysis performed on the band-pass filtered satellite SSH indicates that the second baroclinic mode may also involves in the eastward-propagating signals observed along the equator. The results are in a good agreement with the modeling and observational studies.

Acknowledgment

Valuable discussions with Prof. Toshio Yamagata, Y. Masumoto and T. Tozuka are greatly appreciated. The sea level data are provided by University of Hawaii Sea Level Center. The satellite SSH data made available by the AVISO, and the wind data are obtained from NCEP/NCAR. The wavelet software was provided by C. Torrence and G. Compo and is available at http://paos.colorado.edu/research/wavelets.

References

Arief, D., and S. P. Murray, 1996, Low-frequency Fluctuations in the Indonesian Throughflow Through Lombok Strait, *J. Geophys. Res.*, **101:12**, 455-464.

Chong, J. C., J. Sprintall, S. Hautala, W. Morawitz, N. A. Bray and W. Pandoe, 2000, Shallow Throughflow Variability in the Outflow Straits of Indonesia, *Geophys. Res. Lett.*, **27**, 125-128.

Fu, L. L., 2007, Intraseasonal Variability of the Equatorial Indian Ocean Observed From Sea Surface Height, Wind, and Temperature Data, *J. Phys. Oceanogr.*, **37**, 188-202.

Han, W., 2005, Origins and Dynamics of the 90-day and 30-60 Day Variations in the Equatorial Indian Ocean. *J. Phys. Oceanogr.*, **35**, 708-728.

Han, W., T. Shinoda, L. -L. Fu, J. P. McCreary, 2006, Impact of Atmospheric Intraseasonal Oscillations on the Indian Ocean Dipole During the 1990s. *J. Phys. Oceanogr.*, **36**, 670-690.

Iskandar, I., W. Mardiansyah, Y. Masumoto and T. Yamagata, 2005, Intraseasonal Kelvin Waves Along the Southern Coast of Sumatra and Java, *J. Geophys. Res.*, **110**, C04013.

Iskandar, I., T. Tozuka, Y. Masumoto, and T. Yamagata, 2008, Impact of Indian Ocean Dipole on Intraseasonal Zonal Current at 90°E on the Equator as Revealed by Self-organizing Map, *Geophys. Res. Lett.*, **35**, L14S03.

Luyten, J. R., and D. Roemmich, 1982, Equatorial currents at semiannual period in the Indian Ocean, *J. Phys. Ocenogr.*, **12**, 406-413.

Madden, R. A. and P. R. Julian, 1971, Detection of a 40–50 day oscillation in the zonal wind in the tropical Pacific, *J. Atmos. Sci.*, **28**, 702-708.

Masumoto, Y., H. Hase, Y. Kuroda, H. Matsuura and K. Takeuchi, 2005, Intraseasonal Variability in the Upper Layer Currents Observed in the Eastern Equatorial Indian Ocean, *Geophys. Res. Lett.*, **32**, L02607.

McPhaden, M. J., 1982, Variability in the Central Equatorial Indian Ocean. Part I: Ocean dynamics, *J. Mar. Res.*, **40**, 157-176.

Murtugudde, R. G., J. P. McCreary, and A. J. Busalacchi, 2000, Oceanic Processes Associated with Anomalous Events in the Indian Ocean with Relevance to 1997-1998, *J. Geophys. Res.*, **105**, 3295-3306.

Rao, S. A., and T. Yamagata, 2004, Abrupt Termination of Indian Ocean Dipole Events in Response to Intraseasonal Disturbances. *Geophys. Res. Lett.*, **31**, L19306.

Reppin, J., F. A. Schott, J. Fischer and D. Quadfasel, 1999, Equatorial Currents and Transports in the Upper Central Indian Ocean: Annual Cycle and Interannual variability, *J. Geophys. Res.*, **104:15**, 495-514.

Saji, N. H., B. N. Goswami, P. N. Vinayachandran, and T. Yamagata, 1999, A Dipole Mode in the Tropical Indian Ocean, *Nature*, **401**, 360-363.

Torrence, C., and G. P. Compo, 1998, A Practical Guide to Wavelet Analysis, *Bull. Am. Meteorol. Soc.*, **79**, 61-78.

Vinayachandran, P. N., N. H. Saji, and T. Yamagata, 1999, Response of the Equatorial Indian Ocean to an Unusual Wind Event During 1994. *Geophys. Res. Lett.*, **26**, 1613-1616.

Webster, P. J., A. M. Moore, J. P. Loschnigg, and R. R. Leben, 1999, Coupled Ocean-atmosphere Dynamics in the Indian Ocean During 1997-98, *Nature*, **401**, 356-359.

Wyrtki, K., 1973, An Equatorial Jet in the Indian Ocean, *Science*, **181**, 262-264.